CRACK CHARACTERIZATION BY AN INVERSE SCATTERING METHOD

D. A. Sotiropoulos and J. D. Achenbach

The Technological Institute, Northwestern University, Evanston, IL 60201, U.S.A.

Abstract—Elastic wave scattering data is utilized to characterize a crack of arbitrary shape by an equivalent elliptical crack contained in an unbounded solid. The inverse method is based on an integral representation for the scattered field in the frequency domain. The proposed method is valid for both small and intermediate wavelengths as compared with the size of the crack. In particular for intermediate wavelengths and normal incidence a simple method is discussed. Its solution gives the location of the geometrical center of the crack, the crack size, and the crack-opening displacement.

INTRODUCTION

A crack in the interior of a solid body can be characterized through its measurable effect on an externally applied ultrasonic field. Recent review papers on ultrasonic QNDE which include substantial discussions of scattering of ultrasonic waves by cracks are those of Thompson[1] and Fu[2]. Practical applications have been discussed by Coffey and Chapman[3]. For the theoretical solution of the direct problem of scattering of elastic waves by cracks we point out the papers by Mal[4], Krenk and Schmidt[5], and Martin[6], and the monograph given in Ref. [7].

There is considerable literature on the general inverse scattering problem, particularly for scattering of acoustic and electromagnetic waves, see, e.g. Devaney[8] and DeFacio and Rose[9]. On the inverse problem of scattering by cracks, relatively little has, however, been published. A method based on inverse time-domain ray tracing, has been discussed in Ref. [10]. Teitel[11] and Gubernatis and Domany[12] have discussed the determination of orientation and size for cracks which are elliptical in shape, the location of which are known *a priori*. Their method utilizes scattered data at very large wavelengths as compared with the size of the crack, and is based on the quasi-static crack-opening displacements given by Eshelby[13]. A different method has been proposed recently in Ref. [14] to characterize a crack of general shape, the location of which is not known. This method is also valid at large wavelengths.

In the present study, we propose an inverse method for ultrasonic crack-scattering data to characterize an equivalent elliptical crack in a homogeneous isotropic linearly elastic solid. The method is based on an integral representation for the scattered field in the frequency domain, and in the far-field region. The proposed method is valid for both small and intermediate wavelengths as compared with the size of the crack. In particular, for intermediate wavelengths and normal incidence a simple method is discussed. The method is based on an approximate closed form algebraic representation of the crack-opening displacement. Its solution gives the location of the geometrical center of the crack, the crack size, and the crack-opening displacement.

THEORETICAL PRELIMINARIES

We consider a flat crack of area A, that is the scatterer for an incident pulse of wave motion in an unbounded elastic solid. The problem can conveniently be dealt with in the frequency domain. Hence, the generic problem is one of scattering of a time harmonic incident displacement wave of the general form

$$\mathbf{u}^{\text{in}}(\mathbf{x}) \exp(-\mathrm{i}\omega t) \tag{1}$$

where $\mathbf{u}^{\text{in}}(\mathbf{x})$ is understood to depend on frequency. The term $\exp(-\mathrm{i}\omega t)$ will be omited in the sequel. Both the incident and scattered elastic waves satisfy the homogeneous wave equation

$$C_{ijpq}\left(\frac{\partial^2 u_p}{\partial x_j \partial x_q}\right) + \rho\omega^2 u_i = 0 \tag{2}$$

where C_{ijpq} are the elastic moduli of the solid and ρ is its mass density. Application of Green's theorem gives the following integral representation for the scattered displacement field $u_j^{\text{sc}}(\mathbf{x})$:

$$u_j^{\text{sc}}(\mathbf{x}) = \int_A C_{mkpq} \frac{\partial G_{jp}(\mathbf{x}-\zeta)}{\partial x_q} \Delta u_m(\zeta) n_k \, \mathrm{d}A(\zeta) \tag{3}$$

in which G_{jp} is the tensor Green's function for the elastic wave equation (2)

$$\Delta u_m(\zeta) = u_m^+(\zeta) - u_m^-(\zeta) \tag{4}$$

is the jump in displacement (which is equal to the jump in scattered displacement) across the crack surface, and n_k is the unit vector in the direction of the outward normal to A^-. $\mathbf{x}$ and ζ define two coinciding coordinate systems with the origin at the centroid of A. $\mathbf{x}$ represents points outside A, while ζ represents points inside A. For an isotropic elastic solid, under consideration in this study, we have

$$C_{mkpq} = \lambda\delta_{mk}\delta_{pq} + \mu(\delta_{mp}\delta_{kq} + \delta_{mq}\delta_{kp}) \tag{5}$$

and

$$\mu\frac{\partial G_{jp}(\mathbf{x}-\zeta)}{\partial x_q} = \mu(G_{jp,q}^{\text{L}}(\mathbf{x}-\zeta) + G_{jp,q}^{\text{T}}(\mathbf{x}-\zeta)) \tag{6}$$

where

$$\mu G_{jp,q}^{\text{L}}(\mathbf{x}-\zeta) = -\frac{c_{\text{T}}^2}{c_{\text{L}}^2} k_{\text{L}} G(k_{\text{L}}R) A_{jpq}^{\text{L}} \tag{7}$$

$$\mu G_{jp,q}^{\text{T}}(\mathbf{x}-\zeta) = k_{\text{T}} G(k_{\text{T}}R)\left[A_{jpq}^{\text{T}} + \gamma_q\left(\mathrm{i} - \frac{1}{k_{\text{T}}R}\right)\delta_{jp} \right] \tag{8}$$

$$G(k_\alpha R) = \frac{\exp(\mathrm{i}k_\alpha R)}{4\pi R}, \quad \alpha = \text{L}, \text{T} \tag{9}$$

$$k_{\text{L}} = \frac{\omega}{c_{\text{L}}}, \quad c_{\text{L}}^2 = (\lambda + 2\mu)/\rho \tag{10}$$

$$k_{\text{T}} = \frac{\omega}{c_{\text{T}}}, \quad c_{\text{T}}^2 = \mu/\rho \tag{11}$$

$$A_{jpq}^\alpha = -\gamma_j\gamma_p\gamma_q\left(\mathrm{i} - \frac{1}{k_\alpha R}\right) - \frac{1}{k_\alpha R}\left[1 + \frac{3}{k_\alpha R}\left(\mathrm{i} - \frac{1}{k_\alpha R}\right)\right]\Gamma_{jpq} \tag{12}$$

$$\Gamma_{jpq} = \gamma_j \delta_{pq} + \gamma_p \delta_{jq} + \gamma_q \delta_{jp} - 5\gamma_j \gamma_p \gamma_q \tag{13}$$

$$\gamma_i = (x_i - \zeta_i)/R; \quad R = |\mathbf{x} - \boldsymbol{\zeta}|. \tag{14, 15}$$

The unknown crack-opening displacements, Δu_m, in the integrand of eqn (3) are determined by solving integral equations that result from traction boundary conditions on the crack faces. The general system of equations has been presented by Budiansky and Rice[15], for the direct scattering problem.

Equation (3) takes a simple form if one considers the scattered displacement field in the "far-field" region. It can be shown that under the assumptions

$$\frac{L}{r} \ll 1; \quad (k_T L)\left(\frac{L}{r}\right) \ll \pi \tag{16a,b}$$

in which L is a characteristic length of the crack surface and $r = |\mathbf{x}|$, eqn (3) becomes

$$u_j^{sc}(\mathbf{x}) = C_{mkpq} G_{jp,q}^L(\mathbf{x}) \int_A \Delta u_m(\boldsymbol{\zeta}) n_k \exp\left(-ik_L \boldsymbol{\zeta} \cdot \mathbf{x}/r\right) dA(\boldsymbol{\zeta})$$

$$+ C_{mkpq} G_{jp,q}^T(\mathbf{x}) \int_A \Delta u_m(\boldsymbol{\zeta}) n_k \exp\left(-ik_T \boldsymbol{\zeta} \cdot \mathbf{x}/r\right) dA(\boldsymbol{\zeta}). \tag{17}$$

In previous studies[11, 12, 14] the inverse problem was considered for low frequencies, $k_T r \ll 1$. In Refs [11, 12] the assumption $k_\alpha r \gg 1$ was also made, which is not necessary. For the low frequency range, only the first term in an expansion of the exponential in the integrand of eqn (17) was kept. Reference [14] subsequently solved the non-linear optimization problem for the position of the crack with general shape, for the crack-opening volumes, and for the crack orientation. In the present study, the case under consideration is $k_\alpha L > 1$. This together with eqns (16a) and (16b) gives

$$k_\alpha r \gg 1. \tag{18}$$

Use of this inequality makes $G_{jp,q}^\alpha(\mathbf{x})$ of eqns (7) and (8) particularly simple. In what follows, we shall discuss the method of solution of the inverse problem for two cases separately. The first case, deals with characterizing a crack the orientation of which is also unknown. The solution, though theoretically feasible, is practically not convenient. For this reason, the case of normal incidence is handled separately. A different solution technique is applied that is particularly simple for intermediate frequencies.

INVERSE SOLUTION FOR A CRACK OF UNKNOWN ORIENTATION

We suppose that $u_j^{sc}(\mathbf{x})$ is known (from an ultrasonic test) for several observation points defined by $\mathbf{x}$, the relative locations of which are known, but not their coordinates relative to the origin, which is at the centroid of the crack. The idea is to use eqn (17) at a sufficient number of observation points, so that the location of the centroid of the crack, the crack-opening volumes, the crack orientation, and the crack size (assuming a shape) can be determined. The method of solution begins with an expansion of the exponential in the integrand of eqn (17). This gives

$$u_j^{sc}(\mathbf{x}) = C_{mkpq} G_{jp,q}(\mathbf{x}) V_{mk} + C_{mkpq}[G_{jp,q}^L(\mathbf{x})k_L + G_{jp,q}^T(\mathbf{x})k_T](-ix_l/r)M_{lmk} + \cdots \tag{19}$$

where

$$V_{mk} = \tfrac{1}{2}\int_A [\Delta u_m(\zeta)n_k + \Delta u_k(\zeta)n_m]\, dA(\zeta) \qquad (20)$$

is the symmetric tensor representing the crack-opening volumes, and

$$M_{lmk} = \tfrac{1}{2}\int_A \zeta_l[\Delta u_m(\zeta)n_k + \Delta u_k(\zeta)n_m]\, dA(\zeta) \qquad (21)$$

denotes first moments of the crack-opening volumes. Higher order moments are included in the omitted terms of eqn (19). In Ref. [14], only zero moment terms were kept in eqn (19), since a low frequency range was considered, and the inverse problem was subsequently solved for V_{mk} and x. Here, we shall discuss a method of solution for the inverse problem defined by eqn (19) which includes higher order moment terms.

In terms of the known coordinate system, $x_1x_2x_3$, the orientation of which is known, but not the location of its origin, the scattered displacement field, eqn (19), may be written in vector-matrix form as

$$\{u^{sc}(x)\}_{6\times 1} = [P(x)]_{6\times 48}\{B\}_{48\times 1} \qquad (22)$$

where

$$\{B\}^{T} = [V_{11}V_{12}V_{13}V_{22}V_{23}V_{33}M_{l11}M_{l12}M_{l13}M_{l22}M_{l23}M_{l33}\ldots]^{T} \qquad (23)$$

in which $l = 1, 2, 3$. The scattered displacement vector $\{u^{sc}\}$ has six components considering its real and imaginary parts. Vector $\{B\}$ has 48 components, since M_{lmk} has 36 independent components and V_{mk} has 12 independent components. Equation (22) has a convenient form for solution since $\{B\}$ is independent of the observation point, x. The ith equation of eqn (22) in complex form is

$$u_i^{sc}(x) = [P_{i11}P_{i12}P_{i13}P_{i22}P_{i23}P_{i33}Q_{i11l}Q_{i12l}Q_{i13l}Q_{i22l}Q_{i23l}Q_{i33l}\ldots]\{B\} \qquad (24)$$

in which $l = 1, 2, 3$ and

$$\begin{aligned}
P_{i11} &= (\lambda+2\mu)G_{i1,1} + \lambda(G_{i2,2}+G_{i3,3})\\
P_{i12} &= 2\mu(G_{i1,2}+G_{i2,1})\\
P_{i13} &= 2\mu(G_{i1,3}+G_{i3,1})\\
P_{i22} &= (\lambda+2\mu)G_{i2,2} + \lambda(G_{i1,1}+G_{i3,3})\\
P_{i23} &= 2\mu(G_{i2,3}+G_{i3,2})\\
P_{i33} &= (\lambda+2\mu)G_{i3,3} + \lambda(G_{i1,1}+G_{i2,2}).
\end{aligned} \qquad (25)$$

Also

$$Q_{pjkl} = \tilde{P}_{pjk}(-ix_l/r), \quad l = 1, 2, 3 \qquad (26)$$

where $\tilde{P}_{pjk}$ is given by eqns (25) with the change $G^{L}_{pj,k}k_{L} + G^{T}_{pj,k}k_{T}$ instead of $G_{pj,k}$. We suppose that the left-hand side of eqn (22) is known. The equation then defines a set of six non-linear equations for 51 unknowns (3 components of x, and 48 components of B). To obtain a solution we make the system overdetermined by considering the data u_i^{sc} in nine observation points $(x^1, x^2, \ldots, x^9)$, since the components of vector B are independent of x. Thus we have 54 equations and 51 unknowns. Since B appears linearly in eqn (22), we solve for B in terms of the unknown x^1 by considering the data in eight observation points simultaneously. This gives

$$\{u^{sc}(\mathbf{x}^1)u^{sc}(\mathbf{x}^2)\ldots u^{sc}(\mathbf{x}^8)\}^T_{48\times1} = [L(x^1)]_{48\times48}\{B\}_{48\times1}. \tag{27}$$

This, in turn, yields

$$\{B\} = [L(\mathbf{x}^1)]^{-1}\{u^{sc}(\mathbf{x}^1)u^{sc}(\mathbf{x}^2)\ldots u^{sc}(\mathbf{x}^8)\}^T. \tag{28}$$

Substitution of eqn (28) into eqn (22) for the ninth observation point, $\mathbf{x}^9$, gives

$$\{u^{sc}(\mathbf{x}^9)\} = [P(\mathbf{x}^9)][L(\mathbf{x}^1)]^{-1}\{u^{sc}(\mathbf{x}^1)u^{sc}(\mathbf{x}^2)\ldots u^{sc}(\mathbf{x}^8)\}^T. \tag{29}$$

The solution of the inverse problem has therefore been reduced to the solution of eqn (29). This is a system of six non-linear equations for three unknowns (x^1_1, x^1_2, x^1_3), since the relationship between $\mathbf{x}^1, \mathbf{x}^2, \ldots, \mathbf{x}^9$ is known from the relative position of the instrument that measures the scattered data. The non-linear system of equations can be solved by standard non-linear optimization techniques. The solution so obtained is the unknown $\mathbf{x}^1 = (x^1_1, x^1_2, x^1_3)$. Substitution of $\mathbf{x}_1$ in eqn (28) gives V_{ij} and M_{lij}. Once V_{ij} are known the orientation of the crack can be determined from the transformation rule of a tensor. Furthermore, use of V_{ij} and M_{lij} gives the crack-opening displacements and the size of the crack—having assumed its shape—if an expansion in characteristic functions is used for the crack-opening displacements. More terms in such an expansion can be incorporated if higher order moments are included in eqn (19). This, of course, is necessary as the frequency increases. More terms in eqn (19) means more unknowns to solve for in vector $\mathbf{B}$. This would increase dramatically the number of required observation points where the scattered data has to be known. It does seem therefore that even though theoretically the above method is satisfactory, it presents inconveniences if it is to be applied in practice. For this reason, one more assumption will be made that simplifies the method of solution dramatically.

INVERSE SOLUTION FOR NORMAL INCIDENCE

We consider a plane elastic wave incident normally upon a crack of general shape that is contained in an unbounded elastic isotropic solid. The normal to the crack is along the x_3-axis. Then eqn (17) together with inequality (18) gives for the scattered displacement field

$$u^{sc}_j(\mathbf{x}) = ik_L G(k_L r)\gamma_j\left[\left(\frac{v}{1-v}\right)(\gamma^2_1+\gamma^2_2)+\gamma^2_3\right][I^L_R+iI^L_I]$$

$$-ik_T G(k_T r)\frac{2v}{1-2v}\left[\gamma_j(\gamma^2_1+\gamma^2_2)-\gamma_1\delta_{j1}-\gamma_2\delta_{j2}\right.$$

$$+\left(\frac{1-v}{v}\right)(\gamma_j\gamma^2_3-\gamma_3\delta_{j3})\left.\right][I^T_R+iI^T_I] \tag{30}$$

where

$$\Delta u_3(\zeta) = \Delta u^R_3(\zeta)+i\Delta u^I_3(\zeta) \tag{31}$$

$$I^\alpha_\beta = \int_A \Delta u^\beta_3 \exp(-ik_\alpha\zeta\cdot\gamma)\,dA(\zeta), \quad \alpha = L,T; \quad \beta = R,I \tag{32}$$

$$\gamma_i = x_i/r. \tag{33}$$

In eqn (30) v is Poisson's ratio of the material. We suppose that the scattered data, u^{sc}, is known. Then for one observation point $\mathbf{x}$, eqn (30) defines a set of six non-linear equations and seven unknowns (I^α_β and $\mathbf{x}$). The four unknowns I^α_β, defined by eqn (32), depend on

the observation point x through γ. Since I_β^α appear linearly in eqn (30), they can be obtained in terms of x by simultaneous solution of any four of six equations of eqns (30). The result is

$$[I_R^L I_I^L I_R^T I_I^T]^T = [M]^{-1}[\text{Re }(u_1^{sc}) \text{ Im }(u_1^{sc}) \text{ Re }(u_3^{sc}) \text{ Im }(u_3^{sc})]^T \tag{34}$$

where

$$
\begin{aligned}
M_{11} &= D_{1R}^L, & M_{12} &= -D_{1I}^L, & M_{13} &= D_{1R}^T, & M_{14} &= -D_{1I}^T \\
M_{21} &= D_{1I}^L, & M_{22} &= D_{1R}^L, & M_{23} &= D_{1I}^T, & M_{24} &= D_{1R}^T \\
M_{31} &= D_{3R}^L, & M_{32} &= -D_{3I}^L, & M_{33} &= D_{3R}^T, & M_{34} &= -D_{3I}^T \\
M_{41} &= D_{3I}^L, & M_{42} &= D_{3R}^L, & M_{43} &= D_{3I}^T, & M_{44} &= D_{3R}^T
\end{aligned}
\tag{35}
$$

and

$$
\begin{aligned}
D_{jR}^L &= -k_L \text{ Im } [G(k_L r)]N_1(\gamma_j) \\
D_{jI}^L &= k_L \text{ Re } [G(k_L r)]N_1(\gamma_j) \\
D_{jR}^T &= k_T \text{ Im } [G(k_T r)]N_2(\gamma_j) \\
D_{jI}^T &= -k_T \text{ Re } [G(k_T r)]N_2(\gamma_j)
\end{aligned}
\tag{36}
$$

$$N_1(\gamma_j) = \gamma_j\left[\left(\frac{v}{1-v}\right)(\gamma_1^2+\gamma_2^2)+\gamma_3^2\right]$$

$$N_2(\gamma_j) = \frac{2v}{1-2v}\left[\gamma_j(\gamma_1^2+\gamma_2^2)-\gamma_1\delta_{j1}-\gamma_2\delta_{j2}+\left(\frac{1-v}{v}\right)(\gamma_j\gamma_3^2-\gamma_3\delta_{j3})\right].$$

Substitution of eqn (34) into the remaining two equations of eqn (30) (Re (u_2^{sc}) and Im (u_2^{sc})) gives two non-linear equations and three unknowns (x_1^1, x_2^1, x_3^1). If the same process is repeated for another observation point say, x^2, then two more non-linear equations are obtained. Thus overall we have four non-linear equations and three unknowns x^1, since $x^2 = x^1 + X_{12}$ and X_{12} is known from the relative position of the instrument that measures the scattered data. Standard non-linear optimization techniques can be used to solve the overdeterminate system of equations at hand. The solution so obtained is the unknown x^1. Substitution of x^1 in eqn (34) gives $I_\beta^\alpha(x^1)$. Similarly $I_\beta^\alpha(x^2)$ is also obtained. It should be emphasized here that up to this point no assumption on the crack's shape has been made.

We proceed now to obtain information about the crack-opening displacement and the crack size presuming knowledge of the crack's shape. In what follows, we represent the crack of unknown general shape by an equivalent elliptical crack. Furthermore, its crack-opening displacement for a fixed frequency is written as

$$\Delta u_3^\beta = \sum_{n=0}^M E_n^\beta(1-\zeta_1^2/a^2-\zeta_2^2/b^2)^{(n+1)/2}, \quad \beta = R, I \tag{37}$$

where superscript β refers to real or imaginary parts, a and b (where $a > b$) are the semi-axes of the ellipse, and the constants E_n^β are understood to depend on frequency. Equation (37) of the crack-opening displacement was motivated by the fact that it is particularly useful for intermediate and lower frequencies, $k_T L \lesssim 1.5$. In fact, it is expected that the first term
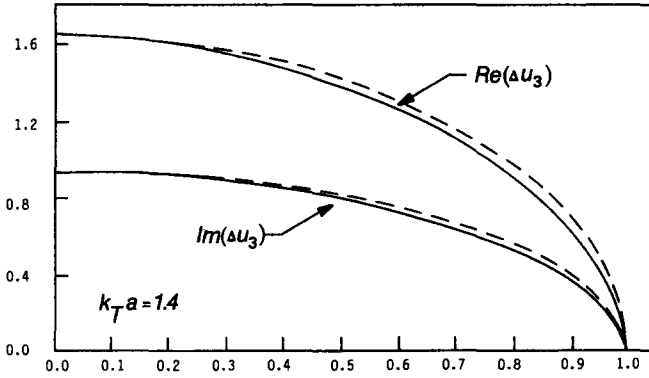
Fig. 1. Comparison of exact crack-opening displacement (solid lines) with approximate one as given by an ellipse (dotted lines). The numbers shown are normalized by $8/\pi u_0(k_L a) (1-v)^2/(1-2v)$.

of eqn (37) will approximate Δu_3^β quite accurately for $k_T L \lesssim 1.5$. In Fig. 1 the "exact" real and imaginary parts of Δu_3 are shown (solid lines) for a penny-shaped crack under normal incidence with $k_T a = 1.4$, as obtained from the numerical solution of the integral equation[16]. A comparison is made with Δu_3^β as given by the first term of eqn (37) (dotted lines). The agreement is good. For higher frequencies more terms in eqn (37) must be kept. Substitution of eqn (37) in eqn (32) and subsequent evaluation of the integral (see Appendix) gives

$$I_\beta^\alpha = \sum_{n=0}^{M} E_n^\beta \pi ab 2^m \Gamma(m) J_m(\kappa_\alpha a) (\kappa_\alpha a)^{-m}, \quad m = (n+3)/2 \tag{38}$$

where

$$\kappa_\alpha = \frac{k_\alpha}{r}\left(x_1^2 + x_2^2 \frac{b^2}{a^2}\right)^{1/2}. \tag{39}$$

The left-hand side of eqn (38) is known from eqn (34). Thus, for each observation point, eqn (38) defines a set of four non-linear equations and $2(M+2)$ unknowns (E_n^β, a, b). The unknowns are determined by considering a number of observation points that is at least equal to the smallest integer that is larger or equal to $(M+2)/2$. The solution can be simply obtained by first considering $2(M+1)$ and solving for the $2(M+1)$ unknowns, E_n^β, that appear linearly in the equations, in terms of a and b. Substitution of E_n^β into at least the two remaining equations defines a non-linear optimization problem for the two unknowns a and b, that can be solved for by a least squares method. For intermediate frequencies ($k_T a \leqslant 1.5$), the solution technique becomes particularly simple, and the solution is obtained in closed form in what follows.

As discussed previously, for $k_T a \lesssim 1.5$ only the first term is kept in eqn (37). Equation (38) then gives

$$I_\beta^\alpha = E^\beta 2\pi ab[\sin (\kappa_\alpha a)/\kappa_\alpha a - \cos (\kappa_\alpha a)]/(\kappa_\alpha a)^2. \tag{40}$$

The functional form of eqn (40) agrees with that of eqns (31) and (32) in the work of Fu[17]. Since $k_T a \lesssim 1.5$ is under consideration we have

$$\kappa_\alpha a < 1.5. \tag{41}$$

This relation simplifies eqn (40) to

$$I_\beta^\alpha = E^\beta 2\pi ab[1 - (\kappa_\alpha a)^2/10]/3, \quad \alpha = \text{L, T.} \tag{42}$$

It appears that eqn (42) defines a set of four independent equations and four unknowns (E^R, E^I, a, b). However, it is noted that

$$I_R^L/I_R^T = I_I^L/I_I^T. \tag{43}$$

Thus eqn (42) gives only three independent equations. To determine the four unknowns, one more equation is needed. This equation is provided by considering another observation point, $\bar{x}$ at the same frequency. Equation (42) then gives

$$\bar{I}_\beta^\alpha = E^\beta 2\pi ab[1 - (\bar{\kappa}_\alpha a)^2/10]/3 \tag{44}$$

where

$$\bar{\kappa}_\alpha = \frac{k_\alpha}{\bar{r}}[\bar{x}_1^2 + \bar{x}_2^2(b/a)^2]^{1/2}. \tag{45}$$

Use of any one of eqns (44) together with any three equations of eqns (42) gives four equations to be solved simultaneously for the four unknowns (E^R, E^I, a, b). As an example, consider

$$\bar{I}_I^T = E^I 2\pi ab[1 - (\bar{\kappa}_T a)^2/10]/3 \tag{46a}$$

$$I_R^L = E^R 2\pi ab[1 - (\kappa_L a)^2/10]/3 \tag{46b}$$

$$I_R^T = E^R 2\pi ab[1 - (\kappa_T a)^2/10]/3 \tag{46c}$$

$$I_I^T = E^I 2\pi ab[1 - (\kappa_T a)^2/10]/3 \tag{46d}$$

the solution of which is obtained as

$$a^2 = \frac{10}{k_T^2}\frac{[I_R^L - I_R^T][r^2\bar{x}_2^2 - Cx_2^2\bar{r}^2]}{[I_R^L - I_R^T(k_L/k_T)^2][x_1^2\bar{x}_2^2 - x_2^2\bar{x}_1^2]} \tag{47}$$

$$(b/a)^2 = \frac{Cx_1^2\bar{r}^2/r^2 - \bar{x}_1^2}{\bar{x}_2^2 - Cx_2^2\bar{r}^2/r^2} \tag{48}$$

where

$$C = \frac{I_I^T - \bar{I}_I^T(1 - R)}{I_I^T R} \; ; \quad R = \frac{I_R^L - I_R^T}{I_R^L - I_R^T(k_L/k_T)^2}. \tag{49}$$

Equations (47) and (48) give the semi-axes $a > b$ of the equivalent elliptical crack. The crack-opening displacement is given by the first term of eqn (37) with E^R, E^I readily obtained from eqns (46) since a and b are known.

APPLICATIONS

Several numerical tests have been performed to check the validity of the solution of the inverse problem. Discussion of the results of one of the tests is given here. The crack considered is penny shaped, and is normal to the propagation direction of an incident plane wave, which is longitudinally polarized along the x_3-direction, with amplitude u^0 and wave number k_L. The crack is contained in an infinite elastic isotropic solid characterized by Poisson's ratio $v = 0.3$.

Table 1. Real and imaginary parts of displacement components for the scattered field at two positions: $x^1/a = (5, 5, 10)$ and $x^2/a = (6, 7, 10)$

$k_T a = 1.4$	x^1/a	x^2/a
u_1^R/u_0	0.025	0.027
u_1^I/u_0	−0.033	0.029
u_2^R/u_0	0.025	0.031
u_2^I/u_0	−0.033	0.033
u_3^R/u_0	0.013	−0.026
u_3^I/u_0	0.041	−0.008

To obtain the position of the centroid of the crack, the crack size and the crack-opening displacement, the scattered displacement field is needed at two observation points. This data is synthesized by first solving the direct problem. The real and imaginary parts of the crack-opening displacement are given in Fig. 1, for $k_T a = 1.4$. Subsequently eqn (30) has been used to obtain the scattered data in the far field. The two observation points chosen arbitrarily are $x^1/a = (5, 5, 10)$ and $x^2/a = (6, 7, 10)$. The scattered particle displacement components at these two observation points, for $k_T a = 1.4$, are listed in Table 1.

The synthesized scattered data was used to solve the inverse problem. The position of one of the observation points was obtained as well as the crack size, and the crack-opening displacement. For a penny-shaped crack and for $k_T a \lesssim 1.5$ the radius of the crack is simply given as

$$a^2 = \frac{10}{k_T^2} \frac{[I_\beta^L - I_\beta^T]}{[I_\beta^L - I_\beta^T(k_L/k_T)^2]} \frac{r^2}{[x_1^2 + x_2^2]} \tag{50}$$

where β is either the real part or the imaginary part. Also, I_β^α is either at x or at $\bar{x}$. The crack-opening displacement follows as

$$\Delta u_3^\beta = E^\beta (1 - r^2/a^2)^{1/2}, \quad \beta = R, I \tag{51}$$

where

$$E^\beta = 3I_\beta^\alpha [1 - (\kappa_\alpha a)^2/10]^{-1}[2\pi a^2]^{-1}. \tag{52}$$

The match between the solution of the inverse problem and the geometrical parameters used to synthesize the scattered data, was found to be excellent, for several frequencies. Numerical tests were also performed on modified scattered data to test the stability of the solution. It should be pointed out here, that different errors in the measured components of the scattered displacement field lead to solutions of eqn (34) that are different from each other depending on which displacement components we used. For this reason, an averaging approach should be taken. Similarly, in solving eqn (42) a different solution is obtained depending on which three equations we consider. Again, it would be appropriate to take the average of all the solutions obtained.

In Fig. 2, a representative example of the stability tests performed is shown. The scattered data used was varied from the exact known data (horizontal axis). The real and imaginary parts of each one of the components of the scattered displacement field were changed by the same amount, while the other components used were the exact ones. The vertical axis of Fig. 2 defines the absolute value of the relative error of the calculated size from the exact known size. It is found that errors in the scattered data cause errors of the same order of magnitude in the inverse solution.
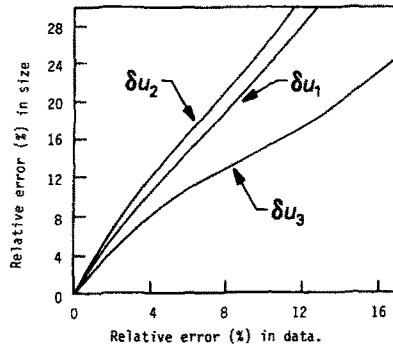
Fig. 2. Relation between crack-sizing error and data error.

REFERENCES

1. R. B. Thompson, Quantitative ultrasound nondestructive evaluation methods. *J. Appl. Mech.* **50** (50th Anniversary Issue), 1191–1201 (1983).
2. L. S. Fu, Mechanics aspects of NDE by sound and ultrasound. *Appl. Mech. Rev.* **35**, 1047–1057 (1982).
3. J. M. Coffey and R. K. Chapman, Application of elastic scattering theory for smooth flat cracks to the quantitative prediction of ultrasonic defect detection and sizing. *Nucl. Energy* **22**, 319–333 (1983).
4. A. K. Mal, Interaction of elastic waves with a penny-shaped crack. *Int. J. Engng Sci.* **8**, 381–388 (1970).
5. S. Krenk and H. Schmidt, Elastic wave scattering by a circular crack. *Phil. Trans. R. Soc. Lond.* **A308**, 167–198 (1982).
6. P. A. Martin, Diffraction of elastic waves by a penny-shaped crack. *Proc. R. Soc. Lond.* **A378**, 262–285 (1982).
7. J. D. Achenbach, A. K. Gautesen and H. McMaken, *Ray Methods for Waves in Elastic Solids—With Applications to Scattering by Cracks.* Pitman, Boston (1982).
8. A. J. Devaney, Fundamental limitations in inverse source and scattering problems in NDE. In *Review of Progress in Quantitative NDE* (Edited by D. O. Thompson and D. E. Chimenti), Vol. 5A, pp. 303–314. Plenum Press, New York (1986).
9. B. DeFacio and J. H. Rose, A perturbation method for inverse scattering in three dimensions based on the exact inverse scattering equations. In *Review of Progress in Quantitative NDE* (Edited by D. O. Thompson and D. E. Chimenti), Vol. 5A, pp. 345–353. Plenum Press, New York (1986).
10. A. N. Norris and J. D. Achenbach, Mapping of a crack edge by ultrasonic methods. *J. Acoust. Soc. Am.* **72**, 264–272 (1982).
11. S. Teitel, Determination of crack characteristics from the quasistatic approximation for the scattering of elastic waves. *J. Appl. Phys.* **49**, 5763–5767 (1978).
12. J. E. Gubernatis and E. Domany, Rayleigh scattering of elastic waves from cracks. *J. Appl. Phys.* **50**, 818–824 (1979).
13. J. D. Eshelby, The determination of the elastic field of an ellipsoidal inclusion and related problems. *Proc. R. Soc. Lond.* **A241**, 376 (1957).
14. J. D. Achenbach, D. A. Sotiropoulos and H. Zhu, Characterization of cracks from ultrasonic scattering data. *J. Appl. Mech.* (1988), in press.
15. B. Budiansky and J. R. Rice, An integral equation for dynamic elastic response of an isolated 3-D crack. *Wave Motion* **1**, 187–192 (1979).
16. J. D. Achenbach and D. Budreck, Personal communication (1986).
17. L. S. Fu, A new micro-mechanical theory for randomly inhomogeneous media, ASME Symposium Wave Prop. Inhomo. Media and Ultrasonic NDE, San Antonio, Texas (1984).

APPENDIX

The integral to be evaluated is written as

$$I = \int_{-b}^{b} e^{-ik\zeta_2 x_2/r} I^*(\zeta_2) \, d\zeta_2 \tag{A1}$$

where

$$I^*(\zeta_2) = \int_{-a(1-\zeta_2^2/b^2)^{1/2}}^{a(1-\zeta_2^2/b^2)^{1/2}} e^{-ik\zeta_1 x_1/r} \, (1-\zeta_1^2/a^2-\zeta_2^2/b^2)^{(n+1)/2} \, d\zeta_1. \tag{A2}$$

With the change of variable $\zeta_1' = \zeta_1/B$, $B = a(1-\zeta_2^2/b^2)$ integral (A2) becomes

$$I^*(\zeta_2) = \frac{B^{n+2}}{a^{n+1}} \int_{-1}^{1} e^{-iBkx_1\zeta_1'/r} (1-\zeta_1'^2)^{(n+1)/2} \, d\zeta_1'. \tag{A3}$$

The integral is recognized as a Bessel function since

$$J_v(z) = \frac{(z/2)^v}{\Gamma(v+1/2)\Gamma(1/2)} \int_{-1}^{1} e^{-izt} (1-t^2)^{v-1/2} \, dt. \tag{A4}$$

Use of eqn (A4) in eqn (A3) gives

$$I^*(\zeta_2) = C(1-\zeta_2^2/b^2)^{(n/2+1)/2}J_{n/2+1}[kx_1a(1-\zeta_2^2/b^2)^{1/2}/r] \tag{A5}$$

where

$$C = \Gamma(1/2)\Gamma(n/2+3/2)a^{-n/2}(kx_1/2r)^{-1-n/2}. \tag{A6}$$

Now, we substitute eqn (A5) into eqn (A1) with $\zeta_2 = b \cos \theta$, and $J_{-1/2}(z) = (2/\pi z)^{1/2} \cos z$ and get

$$I = 2Cb(\pi kx_2b/2r)^{1/2} \int_0^{\pi/2} J_{-1/2}(kx_2b \cos \theta/r)J_{n/2+1}(kx_1a \sin \theta/r) \cos^{1/2} \theta \sin^{n/2+2} \theta \, d\theta. \tag{A7}$$

This is recognized as a Bessel function, since Sonine's second finite integral is

$$\int_0^{\pi/2} J_\mu(z \sin \theta)J_v(Z \cos \theta) \sin^{\mu+1} \theta \cos^{v+1} \theta \, d\theta = \frac{z^\mu Z^v J_{\mu+v+1}\{\sqrt{(Z^2+z^2)}\}}{\{Z^2+z^2\}^{1/2(\mu+v+1)}}; \quad \text{Re}(\mu), \quad \text{Re}(v) > -1. \tag{A8}$$

Use of eqn (A8) in eqn (A7) gives

$$I = \pi ab2^m\Gamma(m)(\kappa a)^{-m}J_m(\kappa a), \quad m = (n+3)/2 \tag{A9}$$

where

$$\kappa = \frac{k}{r}\left[x_1^2 + x_2^2\left(\frac{b^2}{a^2}\right)\right]^{1/2}. \tag{A10}$$